



Contents lists available at ScienceDirect

Optik

journal homepage: [www.elsevier.com/locate/ijleo](http://www.elsevier.com/locate/ijleo)

Original research article

# Study of high beam quality side-pumped Nd:YLF laser with intracavity Gaussian aperture

Qin Dai, Shanchun Zhang, Yequ Li, Jianfeng Cui, Ribo Ning, Rina Wu\*

School of science, Shenyang Ligong University, Shenyang, 110159, China

## ARTICLE INFO

## Keywords:

Beam quality  
Gaussian aperture  
YLF laser

## ABSTRACT

In order to obtain a 1053 nm output laser with a high beam quality, the mode distribution of the YLF solid laser with a plane-plane resonator is studied. According to the Collins theory, the influences of the position and size parameters of a Gaussian aperture on the mode of the output beam is simulated and analyzed. Compared with the simulation results without a Gaussian aperture, the Gaussian aperture in the cavity can significantly improve the quality of the output laser. Based on the theoretical simulations, a laser with optimal structural parameters is built. The profiles and mode distributions of the laser output beams with a Gaussian aperture and without a Gaussian aperture in the cavity are measured, respectively. When the radius of the light spot on the film of the Gaussian aperture is 4 mm and the distance between the Gaussian aperture and total-reflection mirror is 30 mm, a 1053 nm laser output with the values of  $M^2$  in the x and y directions of 1.9 and 1.8, and maximum output power of 9.7 W is obtained. The experimental results demonstrate that the Gaussian aperture in the cavity can improve the mode distribution of the cavity and obtain the laser output with a higher beam quality, which is basically consistent with the results of theoretical simulations.

## 1. Introduction

Nd:YLF crystal is effective in energy storage under the same pumping conditions due to its long fluorescence lifetime in physical properties. The thermal-induced birefringence of this crystal is smaller than the natural birefringence, so that it could reduce the thermal-induced depolarization effect [1–7]. However, the YLF crystal, as an anisotropic material, has different stress coefficients in various directions of the crystal. Hence, the wavefront thermal distortion becomes an irregular distortion, which seriously affects the beam quality of the output laser. When the inhomogeneous stress distribution exceeds a certain limitation, cracks are prone to occur in the crystal.

In order to take the full advantages of a YLF solid-state laser, many scholars have studied Nd:YLF crystal in detail. Ma et al. used laser diode (LD)-pumped end-face a-axis tangential Nd:YLF slats to generate a 1053 nm laser with  $M^2$  of 1.02 and pulse energy of 5 mJ under a continuous pump power of 30 W [8]. Lu et al. obtained a 527 nm laser output with  $M_x^2$  of 1.28,  $M_y^2$  of 1.12 and single pulse energy of 11 mJ based on the structure of an intracavity frequency doubling under the repetition frequency of 500 Hz and pumping energy of 49.8 mJ/pulse [9]. Lu also optimized the efficiency of the mode matching by inserting a cylindrical lens into the cavity to achieve a 523.5 nm green light with  $M^2$  less than 2.5 and single pulse energy of 16.8 mJ under the condition of 500 Hz electro-optic Q-switching [10]. Zhang et al. adopted a 880 nm pumping light to pump an end-face Nd:YLF module, in which a cylindrical lens was added to compensate the thermal effect in the a-axis YLF crystal [11]. A 1047 nm laser with  $M_x^2$  of 1.74,  $M_y^2$  of 1.97 and single pulse

\* Corresponding author.

E-mail address: [wurina2007@126.com](mailto:wurina2007@126.com) (R. Wu).<https://doi.org/10.1016/j.ijleo.2018.09.141>

Received 25 July 2018; Accepted 24 September 2018

0030-4026/© 2018 Elsevier GmbH. All rights reserved.

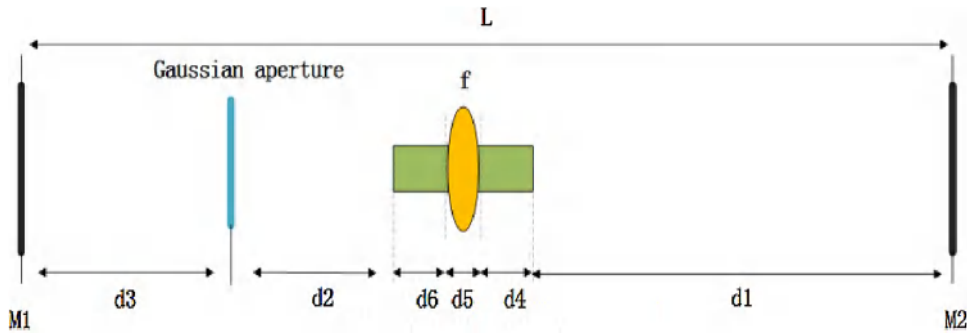


Fig. 1. Schematic diagram of the proposed laser structure.

energy of 9.5 mJ was realized when a 40% transmitting output mirror was used and the focal length of the cylindrical lens was chosen to be 300 mm. Men et al. studied the flash-pumped electro-optic Q-switched dual-wavelength Nd:YLF laser, in which 1047 nm and 1053 nm lasers with a single pulse width of 17 ns and maximum output pulse energies of 66.2 mJ and 83.9 mJ are simultaneously achieved [12]. In summary, the end-face LD-pumped YLF crystal has been extensively investigated. The end-pumping mode could achieve a highly effective mode matching between the pump light and oscillating light, and the output mode is nearly a Gaussian distribution. The side-pumped structure could handle a higher LD pumping power. However, the intracavity mode-matching is inefficient, the mode resolution is poor, and a multi-mode oscillation is easier to form in the cavity.

In this paper, the diode-side-pumped a-axis Nd:YLF laser with a Gaussian aperture is studied. Based on the Collins theory, the influences of the position and size parameters of the Gaussian aperture in the cavity on the output beam mode is simulated and compared with the simulations without a Gaussian aperture. Optimized structural parameters are applied to the laser, and the mode distribution of the output beam is investigated. The experimental results demonstrate that the beam quality is effectively improved with the help of the Gaussian aperture.

## 2. Theoretical simulation

Fig. 1 exhibits a simplified diagram of the proposed laser structure, in which the plane reflector M1, Gaussian aperture, crystal rod and plane output mirror M2 are aligned in the cavity in sequence.  $f$  is the focal length of the equivalent thermal lens in the crystal rod.

We take the output mirror M2 as a reference surface. According to the Collins formula, the electric field amplitude from M2 to the Gaussian aperture is:

$$E_2(r_2, \theta_2) = -\frac{i \exp[ik(L - d3)]}{\lambda B1} \int_0^{2\pi} \int_0^a E_1(r_1, \theta_1) \times \exp\left\{ [A1r_1^2 - 2r_1r_2 \cos(\theta_1 - \theta_2) + D1r_2^2] \frac{ik}{2B1} \right\} r_1 d\theta_1 dr_1 \tag{1}$$

where  $r_1, r_2, \theta_1$  and  $\theta_2$  are the radial and angular parameters of the output mirror M2 and Gaussian aperture, respectively,  $a$  represents the radius of the output mirror,  $k$  is the wavenumber,  $E_1(r_1, \theta_1)$  is the initial distribution of the electric field at the output mirror, and  $A1, B1$  and  $D1$  are one-way matrix elements of the beam passing from M2 to the Gauss aperture.

After integrating  $\theta_1$ , Eq. (1) can be expressed as:

$$E_2(r_2) = -\frac{2\pi i \exp[ik(L - d3)]}{\lambda B1} \exp\left(\frac{ikD1r_2^2}{2B1}\right) \times \int_0^a E_1(r_1) \exp\left(\frac{ikA1}{2B1} r_1^2\right) \times J_0\left(\frac{kr_2r_1}{B1}\right) r_1 dr_1 \tag{2}$$

where  $J_0$  is a zero-order Bessel function and the transformation formula used in the transformation process of Eq. (1) is:

$$\frac{1}{2\pi} \int_0^{2\pi} \exp\left[\frac{ik}{B1} r_1 r_2 \cos(\theta_1 - \theta_2)\right] d\theta_1 = J_0\left(\frac{kr_2r_1}{B1}\right) \tag{3}$$

By the same way, electric fields  $E_3(r_3)$  from the Gaussian aperture to M1,  $E_4(r_2)$  from M1 to the Gaussian aperture, and  $E_5(r_1)$  from the Gaussian aperture to M2 can be obtained as the following equations:

$$E_3(r_3) = -\frac{2\pi i \exp(ikd3)}{\lambda B2} \exp\left(\frac{ikD2r_3^2}{2B2}\right) \times \int_0^b E_2(r_2) \exp\left(\frac{ikA2}{2B2} r_2^2\right) \exp\left(-\frac{r_2^2}{b^2}\right) \times J_0\left(\frac{kr_2r_3}{B2}\right) r_2 dr_2 \tag{4}$$

$$E_4(r_2) = -\frac{2\pi i \exp(ikd3)}{\lambda B2} \exp\left(\frac{ikD2r_2^2}{2B2}\right) \times \int_0^a E_3(r_3) \exp\left(\frac{ikA2}{2B2} r_3^2\right) \times J_0\left(\frac{kr_2r_3}{B2}\right) r_3 dr_3 \tag{5}$$

$$E_5(r_1) = -\frac{2\pi i \exp[ik(L - d3)]}{\lambda B3} \exp\left(\frac{ikD3r_1^2}{2B3}\right) \times \int_0^b E_2(r_2) \exp\left(\frac{ikA3}{2B3} r_2^2\right) \exp\left(-\frac{r_2^2}{b^2}\right) \times J_0\left(\frac{kr_2r_1}{B3}\right) r_2 dr_2 \tag{6}$$

where  $b$  is the radius of the light spot on the film of the Gaussian aperture,  $A_2, B_2$  and  $D_2$  are one-way matrix elements when the beam is transmitted from the Gaussian aperture to M1, and  $A_3, B_3,$  and  $D_3$  are one-way matrix elements when the beam is transmitted from the Gaussian aperture to M2.

According to the finite element subdivision of the reference plane, Eqs. (1), (4)–(6) can be expressed as:

$$E_2(n) = \sum_{m=0}^M T_1 E_1(m) \tag{7}$$

$$E_3(p) = \sum_{n=0}^M T_2 E_2(n) \tag{8}$$

$$E_4(n) = \sum_{p=0}^M T_3 E_3(p) \tag{9}$$

$$E_5(m) = \sum_{n=0}^M T_4 E_4(n) \tag{10}$$

where  $M$  is the total number of finite element meshes, and  $m, n,$  and  $p$  are finite element ordinal number.

$T_1, T_2, T_3$  and  $T_4$  can be obtained as follows:

$$T_1 = -\frac{2\pi i \exp(ik(L - d_3))}{\lambda B_1} \times \exp\left(\frac{ikD_1 a^2 n^2}{2B_1 M^2}\right) \times \exp\left(\frac{ikA_1 a^2 m^2}{2B_1 M^2}\right) \times J_0\left(\frac{ka^2 mn}{B_1 M^2}\right) \frac{a^2 m}{M^2} \tag{11}$$

$$T_2 = -\frac{2\pi i \exp(ikd_3)}{\lambda B_2} \times \exp\left(\frac{ikD_2 b^2 p^2}{2B_2 M^2}\right) \times \exp\left(\frac{ikA_2 b^2 n^2}{2B_2 M^2}\right) \times \exp\left(-\frac{n^2}{M^2}\right) \times J_0\left(\frac{kb^2 np}{B_2 M^2}\right) \frac{b^2 n}{M^2} \tag{12}$$

$$T_3 = -\frac{2\pi i \exp(ikd_3)}{\lambda B_2} \times \exp\left(\frac{ikD_2 a^2 p^2}{2B_2 M^2}\right) \times \exp\left(\frac{ikA_2 a^2 p^2}{2B_2 M^2}\right) \times J_0\left(\frac{ka^2 pn}{B_2 M^2}\right) \frac{a^2 p}{M^2} \tag{13}$$

$$T_4 = -\frac{2\pi i \exp(ik(L - d_3))}{\lambda B_3} \times \exp\left(\frac{ikD_3 b^2 m^2}{2B_3 M^2}\right) \times \exp\left(\frac{ikA_3 b^2 n^2}{2B_3 M^2}\right) \times \exp\left(-\frac{n^2}{M^2}\right) \times J_0\left(\frac{kb^2 mn}{B_3 M^2}\right) \frac{b^2 n}{M^2} \tag{14}$$

Hence, the total transmission matrix  $T$  of one round-trip in the cavity is:

$$T = T_1 T_2 T_3 T_4 \tag{15}$$

When the beam travels in the cavity for sufficient times, it generates self-reproduction, which is:

$$TE_1(r_1) = \lambda E_1(r_1) \tag{16}$$

where  $\lambda$  is the eigenvalue, which is a coordinate-independent complex number describing the attenuation of the amplitude and phase.

Based on the theory above, the mode distribution of the output beam without a Gaussian aperture is simulated and analyzed. In the simulation, the radius of M1 and M2 is set to be 12.5 mm, the length of the cavity is 450 mm, the focal length of the thermal lens is 4000 mm,  $\lambda$  is 1053 nm, the distances from the thermal lens to M2 and M1 are 275 mm and 175 mm, respectively, and the length of the crystal is 150 mm.

Fig. 2 shows the simulated distribution of the mode and profile of the output beam without a Gaussian aperture in the cavity. It can be observed that the output mode is relatively smooth in the middle region, whereas, multiple higher-order modes with lower mode resolutions appear in the edge region, and the output beam is not an ideal Gaussian distribution.

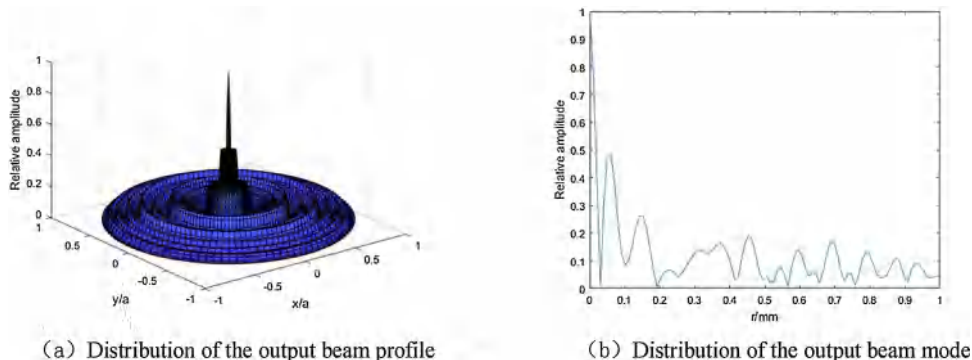


Fig. 2. Simulated distribution of the output beam profile and mode without a Gaussian aperture.

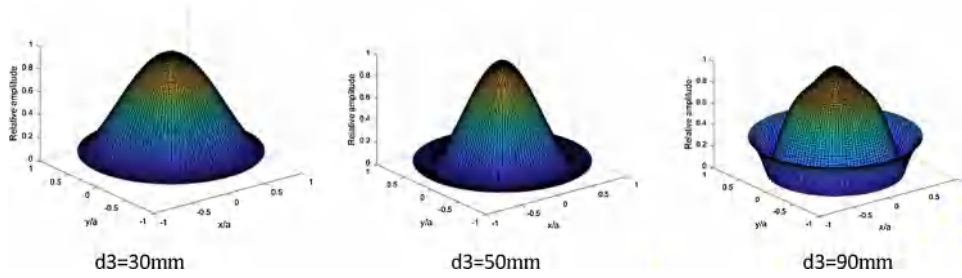


Fig. 3. Three simulated dimensional profiles of the output beam. The Gaussian aperture is placed to 30. mm, 50 mm and 90 mm from M1.

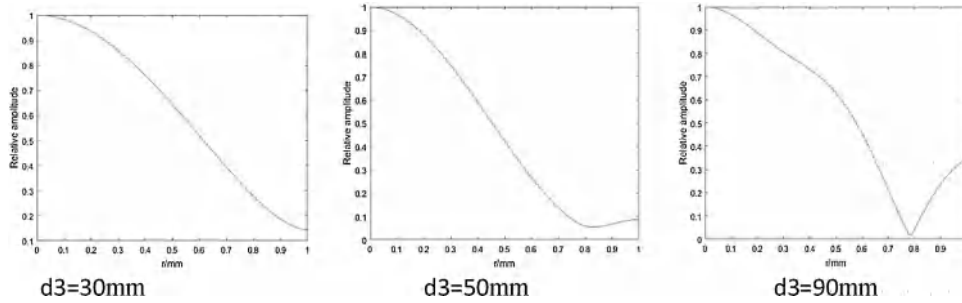


Fig. 4. Simulated distributions of the output beam modes. The Gaussian aperture is placed to 30 mm, 50 mm and mm from M1.

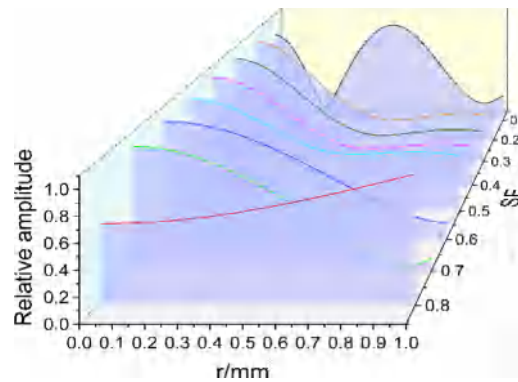


Fig. 5. Distribution of output modes in different SFs.

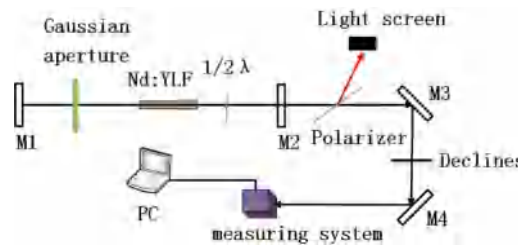


Fig. 6. The diagram of laser structure.

The distributions of the output beam with a Gaussian aperture are also simulated as shown in Figs. 3 and 4. In the simulations, the distances between the Gaussian aperture to M1 are set to be 30 mm, 50 mm and 90 mm, respectively, the outer radius of the Gaussian aperture is 10 mm, the radius of the light spot on the film of the Gaussian aperture is 4 mm, and the distance between M2 and right side of the crystal bar is 200 mm. The output mode shows a smooth and uniform Gaussian distribution when the Gaussian aperture is 30 mm from M1. When the distance is 50 mm, a slight fluctuation appears in the edge area of the output mode, which becomes stronger when the distance is 90 mm.

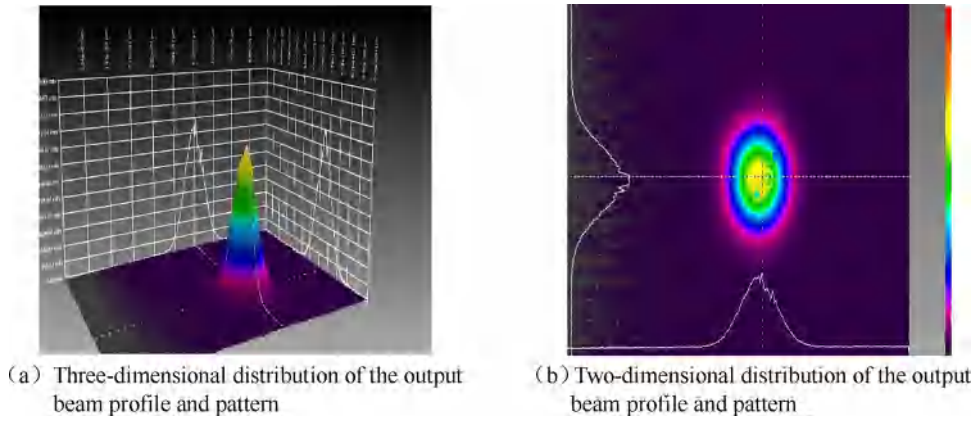


Fig. 7. Distributions of the output beam profile and pattern without a Gaussian aperture.

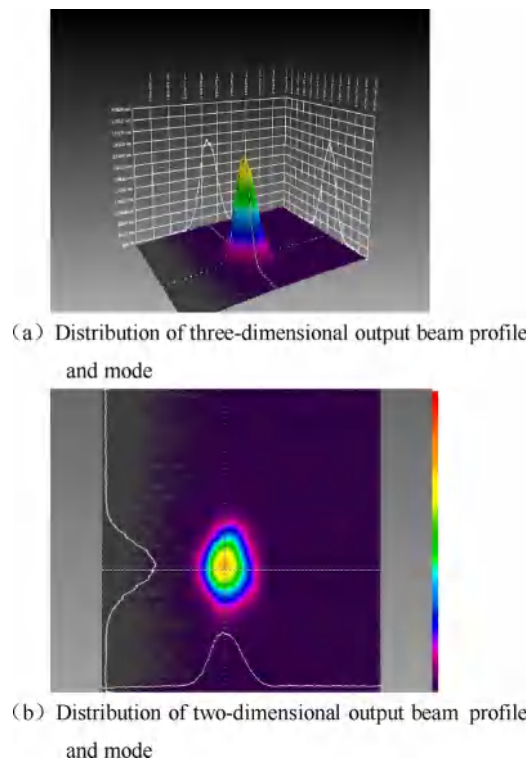


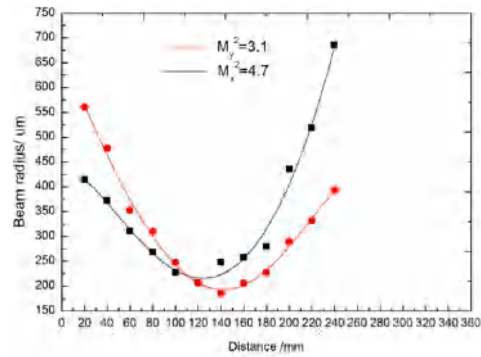
Fig. 8. Distributions of the output beam profile and mode with a Gaussian aperture.

Soft factor (SF), as the ratio of the distance between the light spot and the outer Gaussian aperture to the outer Gaussian aperture radius, can be described as :

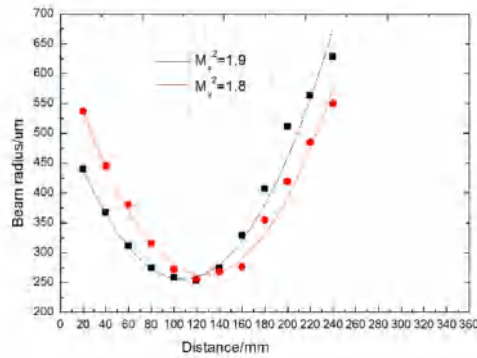
$$SF = \frac{c - b}{c} \tag{17}$$

where c is the outer Gaussian aperture radius, b is the radius of the light spot on the film of the Gaussian aperture.

The distributions of the output mode in different SFs are also simulated as shown in Fig. 5. When SF is 0.8, the beam mode shows a Gaussian hollow distribution. When SF is 0.1, the beam mode presents a strong fluctuation. The mode presents a Gaussian distribution when SF is 0.6 (b is 4 mm), which will significantly improve the quality of output beam and suppress the generation of high-order modes compared to a cavity without a Gaussian aperture.



(a)  $M^2$  curves of a 1053nm beam without a Gaussian aperture



(b)  $M^2$  curves of a 1053nm beam with a Gaussian aperture

Fig. 9. Experimental measured  $M^2$  curves of the output beams.

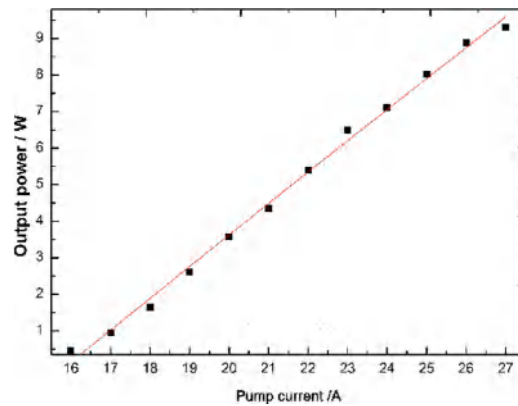


Fig. 10. Dependence of the output power on the pump current.

### 3. Experimental test

Fig. 6 exhibits the structure of the experimental setup, in which the YLF crystal with a size of 3 mm × 150 mm is cut in a-axis, the radii of the plane reflector M1 and plane output mirror M2 are both 12.5 mm, M3 and M4 are reflecting mirrors at 1053 nm, the plane-plane resonator length is 450 mm, the radius of the light spot on the film of the Gaussian aperture is 4 mm, the outer radius of Gaussian aperture is 10 mm, and the distance between the Gaussian aperture and M1 is 30 mm.

Figs. 7 and 8 show two-dimensional and three-dimensional distributions of the output beam mode and profile without a Gaussian aperture and with a Gaussian aperture, respectively, which are measured by a Beam analyzer (Spiricon, BM-USB-SP620). The

distance between the center of the YLF crystal and M1 is 175 mm in Fig. 7 and the distance between the Gaussian aperture and M1 is 30 mm in Fig. 8. Both cases have an output power of 8 W at 1053 nm.

Compared to Fig. 7, Fig. 8 shows that the Gaussian aperture efficiently suppresses the generation of higher-order modes and significantly improves the quality of the output laser beam.

In experiments, a beam measuring instrument (DUMA,  $M^2$  Beam) is used to measure the  $M^2$  values of the output lasers. As shown in Fig. 9,  $M^2$  values of the output beam without a Gaussian aperture in the directions of X and Y planes are 4.7 and 3.1, respectively, which decrease to 1.9 and 1.8 for an output beam with a Gaussian aperture. The Gaussian aperture in the cavity effectively improves the beam quality of the output laser.

Fig. 10 shows the dependence of the output power of 1053 nm on the pump current when a Gaussian aperture is inserted into the cavity. The threshold current of the laser is around 16 A. When the pump current increases to 27 A, the output power of the laser reaches its maximum value of 9.7 W.

#### 4. Summary

The characteristics of the beam mode of an LD-side-pumped YLF solid-state laser with a Gaussian aperture are studied. The influences of the position and size parameters of the Gaussian aperture on the characteristics of output laser are theoretically analyzed by using the Collins theory. Based on the theoretical simulation results, a laser with optimal structural parameters is built. The mode distributions of the output beams with or without a Gaussian aperture are compared. The experimental results demonstrated that the Gaussian aperture in the cavity could significantly improve the output beam quality of LD-side-pumped YLF lasers. A high beam quality output laser with an  $M_x^2$  of 1.9 and  $M_y^2$  of 1.8 is obtained when the radius of the light spot on the film of the Gaussian aperture is 4 mm and the distance between the Gaussian aperture and M1 is 30 mm. The maximum output average power is 9.7 W at 1053 nm.

#### Acknowledgments

This work is supported by the National Natural Science Foundation of China (No. 61705145), Support program for innovative talents in Liaoning University (No. LR2016079), Natural Science Foundation of Liao-ning Province of China No. 201602649, 201801926), Shenyang science and technology plan project (No. 17- 33-6-00).

#### References

- [1] J. Zhang, J. Xia, X. Fu, P. Zhai, Quasi-three-level orthogonally polarized cw dual-wavelength operation in Nd:LiYF<sub>4</sub>, *Opt. Laser Technol.* 90 (2017) 185–189.
- [2] Liu Guohong, Li Yongmin, Wang Yaoting, Li Yuanji, Zhang Kuanshou, All solid state continuous wave stabilized single frequency 1053-nm Nd:YLF laser, *Chin. J. Lasers* 36 (7) (2009) 1733–1734.
- [3] S. Xu, S. Gao, A new wavelength laser at 1370nm generated by Nd:YLF crystal, *Mater. Lett.* 183 (2016) 451–453.
- [4] R.M. El-Agmy, N. Al-Hosiny, Thermal analysis and experimental study of end-pumped Nd:YLF laser at 1053nm, *Photonic Sens.* 7 (4) (2017) 1–7.
- [5] Yang, Xiaolei, Jian, Tingting, Xiuhua, Diode-pumped Nd:YLF slab master oscillator power amplifier laser system with 655 mJ output at 50Hz repetition rate, *Chin. Opt. Lett.* 13 (6) (2015) 44–47.
- [6] Q. Yang, X. Zhu, J. Ma, T. Lu, X. Ma, W. Chen, High energy 523nm ND:YLF pulsed slab laser with novel pump beam waveguide design, *Opt. Commun.* 354 (2015) 414–418.
- [7] Q.S. Qiu, Z.W. Fan, X.X. Tang, L.Q. Hou, Y.L. Liu, High-efficiency electro-optical cavity-dumped Nd:YLF laser with double end-pumping, *J. Optoelectron. Laser* 22 (7) (2011) 961–964.
- [8] Q. Ma, H. Mo, J. Zhao, High-energy high-efficiency Nd:YLF laser end-pump by 808nm diode, *Opt. Commun.* 413 (2018) 220–223.
- [9] Lu Tingting, Juntao Wang, Minjie Huang, Dan Liu, Xiaolei Zhu, Efficient and compact diode-end-pumped conductivity cooled Q-switched Nd:YLF laser operating at 527nm, *Chin. Opt. Lett.* 10 (8) (2012) 36–38.
- [10] T.T. Lu, J. Ma, M.J. Huang, Q. Yang, X.L. Zhu, High-efficient Nd:YLF Q-Switched laser operating at 523.5nm, *Chin. Phys.* 31 (7) (2014) 74208-074208.
- [11] Z. Zhang, Q. Liu, M. Nie, E. Ji, M. Gong, 880-nm-diode- laser-end-pumped electrooptically Q-Switched Nd:YLF laser with high energy and good beam quality at 1047 nm and 1kHz, *IEEE Photonics J.* 8 (1) (2016) 1–8.
- [12] S. Men, Z. Liu, Z. Cong, Y. Li, X. Zhang, Electro-optically Q-switched dual-wavelength Nd:YLF laser emitting at nm and 1053nm, *Opt. Laser Technol.* 68 (2015) 48–51.